Magn Reson Mater Phy (2011) 24:331–337
DOI 10.1007/s10334-011-0273-8

RESEARCH ARTICLE

Stripline resonator and preamplifier for preclinical magnetic resonance imaging at 4.7 T

Ioannis Lavdas · Hugh C. Seton · Charles R. Harrington · Claude M. Wischik

Received: 3 March 2011 / Revised: 30 June 2011 / Accepted: 1 July 2011 / Published online: 4 August 2011

Abstract
Object To design and evaluate a fully shielded, $\lambda/4$ stripline resonator as a receive-only surface coil for preclinical MRI at 4.7 T.
Materials and methods A 20 mm diameter stripline surface coil was fabricated from double-sided Duroid 5880 PCB material and was directly coupled to the input of a MOSFET preamplifier, without requiring a matching network. The new coil was compared with a conventional 20 mm, wire loop, receive-only surface coil in imaging experiments with a separate transmit-only saddle coil.
Results The stripline surface coil exhibits a loaded Q-factor of 132 at 200 MHz, compared to 138 for a conventional wire loop coil and its resonant frequency drops by 0.2 MHz under loading, rather than 0.5 MHz for the wire loop. The stripline coil displays a more symmetrical B_1 map compared to the wire loop, but the SNR falls off more rapidly with depth so it is 30% poorer 8 mm from the coil plane. It should be possible, however, to reduce this difference by using a thicker dielectric in future versions of the stripline coil.
Conclusion Compared to a conventional surface coil, the stripline coil is easy to manufacture, requires shorter set-up times and shows reduced dielectric interaction with conductive samples.

Keywords Preclinical MRI · Surface coil · Stripline resonator · High input impedance preamplifier · Electronic decoupling

I. Lavdas (✉)
Comprehensive Cancer Imaging Centre (CCIC),
Imperial College MRC Cyclotron Building,
Hammersmith Hospital, DuCane Road,
London, W12 0NN, UK
e-mail: ilavdas@imperial.ac.uk

I. Lavdas · H.C. Seton
BioMedical Physics, School of Medical Sciences,
University of Aberdeen, Foresterhill,
Aberdeen, AB25 2ZD, UK

C.R. Harrington · C.M. Wischik
School of Medicine and Dentistry,
University of Aberdeen and TauRx Therapeutics Ltd.,
Foresterhill, Aberdeen, AB25 2ZD, UK

Introduction

We have developed a receive-only surface coil based on a planar transmission line resonator (TLR) for use in a 4.7 T preclinical MRI system (Surrey Medical Imaging Systems, UK). Previously, TLR surface coils fabricated from coaxial cables have been proved effective in reducing de-tuning and de-matching effects in the presence of conductive samples [1], as have surface coils and coil arrays based on microstrip transmission lines, using lumped tuning and matching elements [2–11]. The aim of this study was to develop a robust and reproducible surface coil design, based on a fully shielded stripline transmission line which, in contrast to already published configurations, does not require lumped tuning and matching elements and controls. The new stripline surface coil was manufactured using readily available printed circuit board (PCB) techniques and materials and to our knowledge the particular coil geometry and fabrication method has not been described before.

Theory

The stripline transmission line

The stripline transmission line is commonly used in radio-frequency (RF) and microwave communications [12] and has

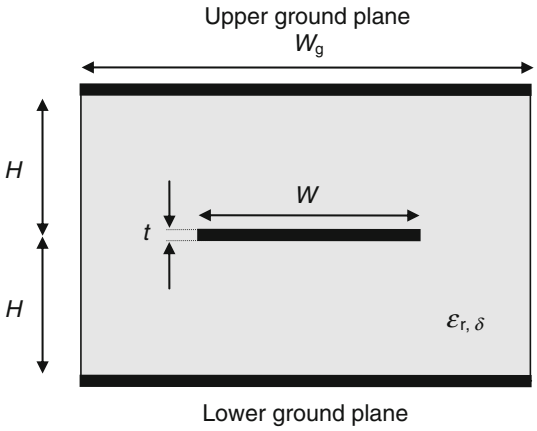

Fig. 1 Stripline configuration

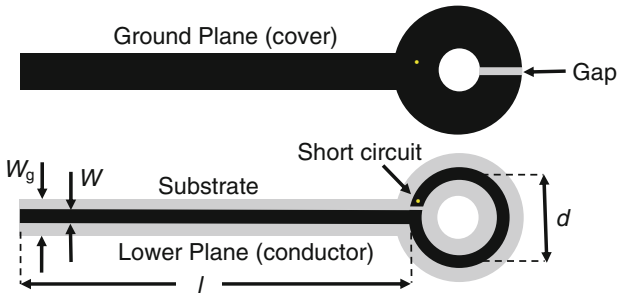

Fig. 2 Design and construction details of the stripline surface coil. The copper layer is represented in *black* and the dielectric substrate in *grey*

useful self-shielding properties that help to minimise stray capacitance effects. In its most common form it consists of a main conductor, usually copper, of width W and thickness t, which is separated from two symmetrical ground planes of width W_g. The dielectric substrate of thickness $2H$, is characterised by its relative permittivity ε_r and loss tangent δ, as shown in Fig. 1.

A stripline can confine electromagnetic energy and allow it to propagate in the dielectric substrate as a transverse electric magnetic (TEM) wave [13]. It thus behaves in a similar way to a coaxial cable, but with the advantage that it can be very easily manufactured on a substrate as a part of a planar circuit, using PCB techniques. Planar RF coil designs incorporating this construction should exhibit very little electrical interaction with nearby conductive samples, helping to minimise de-tuning effects and dielectric losses in NMR and MRI experiments [14].

Quarter wavelength ($\lambda/4$) stripline resonator

If a quarter wavelength ($\lambda/4$) stripline is short-circuited at one end, the distributed capacitance, inductance and losses form a parallel *LCR* resonant circuit. The impedance at the open side of a shorted $\lambda/4$ line is very high, so a coil based on this design can be connected directly to the input of a high impedance preamplifier without the need for a matching network [1]. The quality factor Q of the $\lambda/4$ stripline resonator is heavily dependent on the loss tangent δ of the dielectric material and on the geometry, but is largely unaffected by radiation losses [13]. As a general rule, the Q-factor increases as the loss tangent δ is reduced and it has been also shown that the Q-factor increases with the ratio W/H, shown in Fig. 1, for a given H, but ratios greater than 4 do not result in significant further improvements [12,13]. The unloaded Q-factor of a stripline resonator can be further increased by increasing the spacing between the two ground planes $2H$, but care should be taken to maintain the TEM mode of propagation [13].

Materials and methods

The stripline surface coil

The stripline surface coil was fabricated in two pieces, as shown in Fig. 2, from double-sided, copper-clad PCB material (RT/duroid 5880, Rogers Corporation, USA), using a computer-controlled milling machine (Protomat 93S, LPKF, Garbsen, Germany). RT/duroid 5880 is designed for high frequency applications [15], and is formed from glass-fibre reinforced PTFE with thickness $H = 0.8$ mm, relative permittivity $\varepsilon_r = 2.2$, loss tangent $\delta = 0.0004$ and is copper-clad to a thickness $t = 35\,\mu$m. The low loss tangent of the Duroid suggests that coils made from this material will display low dielectric losses relative to those made from standard FR4 PCB materials and therefore will have relatively high Q-factors, thus yielding good SNR in MRI experiments [14].

The conductor has the form of a straight section of width W and length l ending in a loop of diameter d, isolated by a 0.2 mm-wide milled gap. The total length of the conductor, $l + \pi d$, is made equal to a quarter wavelength ($\lambda/4$). The open end of the loop is shorted to the ground plane on the reverse face by soldering a 0.5 mm diameter wire through a hole in the substrate and another 0.2 mm-wide gap is milled into the ground plane loop, opposite to the short, to allow magnetic flux to pass through the loop. The stripline was completed with an extra ground layer (cover) to mimic the behaviour of fully shielded coaxial cable TLR surface coils [1]. The cover was milled with the same shape as the conductor plane but without a main conductor so that, when assembled, the conductor is shielded by symmetrically placed ground planes to resemble the form of the stripline configuration, shown in Fig. 1. Wires were soldered between the upper and lower ground planes at 2 cm intervals both to ensure electrical connection between the ground planes and to provide mechanical rigidly. The design shown in Fig. 2 was fabricated with $W = 3$ mm, $W_g = 7$ mm, $d = 20$ mm and $l = 140$ mm, resulting in a resonator with a characteristic impedance $Z_0 = 27\,\Omega$ [13]. Once completed the coil was coated with polyurethane varnish (CPL, Electrolube,

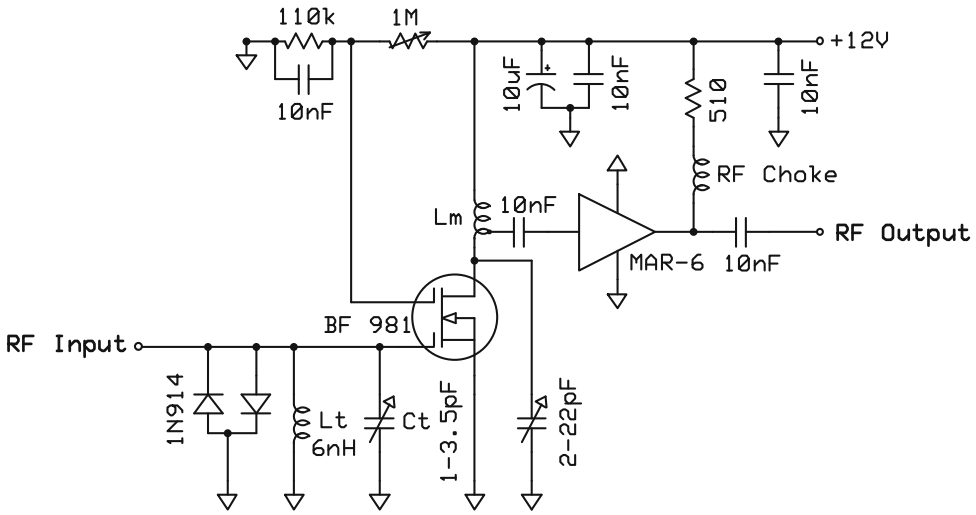

Fig. 3 The high input impedance MOSFET preamplifier developed for use with the stripline surface coil

UK) to prevent oxidation of the copper surfaces and to make cleaning easier. Then the coil was tuned to approximately 200 MHz by observing the resonant frequency, with a coupling loop connected to the reflection port of a network analyser (8712C, Agilent Technologies, USA) and cutting to length. As expected, the resonant frequency increased as the resonator was shortened [12].

The stripline surface coil is expected to exhibit a high loaded Q-factor compared to standard wire loop designs because the electric field is more fully contained by the dielectric substrate, so that dielectric losses due to conductive samples should be greatly reduced [1]. At RF frequencies the dielectric losses are small compared to the coil losses [13], especially when using a material such as Duroid 5880, which has a very small loss tangent ($\delta = 0.0004$). The dielectric substrate of the cover also serves as a spacer between the main conductor and sample giving a "lift-off effect" that helps to maintain the SNR in the presence of remaining magnetically coupled losses [16].

The high-input impedance MOSFET preamplifier

The new stripline surface coil was directly coupled to a low noise, high input impedance RF preamplifier, shown in Fig. 3. The preamplifier, based on a dual-gate MOSFET (BF981, Philips/NXP Netherlands) and similar to published designs, delivers a noise figure of 0.7 dB at 200 MHz [17,18]. The inductor L_t at the input stage compensates for the input capacitance of the MOSFET and the trimmer capacitor C_t (Vishay BC components, Taiwan) is then used for fine tuning of the stripline coil. A pair of crossed-diodes (1N914, Microsemi Corporation, USA) protects the MOSFET during transmit pulses, and simultaneously detunes the stripline coil by approximately 70 MHz during transmission, providing passive receiver decoupling. The MAR-6 output stage (Mini-Circuits, USA) is a wideband, monolithic RF amplifier that is used for output stage amplification and has a 50 Ω output impedance which allows direct connection to the MRI system via coaxial cables.

The bias voltage on the upper gate of the MOSFET was adjusted until V_{G2S} was equal to 4 V [18] and the trimmer capacitor at the drain of the MOSFET (2–22 pF) was adjusted until the tuned circuit formed with L_m resonated at 200 MHz, so that the stripline coil and 50 Ω-terminated preamplifier system showed the highest Q-factor when monitored in transmission mode in the network analyser.

Transmit (Tx) coil and active decoupling circuit

Excitation pulses were generated by a 50 mm diameter saddle coil made of copper foil ($L = 110$ nH), which is surrounded by a 200 mm diameter and 230 mm long, slotted RF shield to attenuate external interference [19]. The saddle coil is electrically balanced [14] and connected via a cable trap to minimise common mode shield currents [20]. The cable trap was formed by wrapping a section of the coaxial cable into a 3-turn solenoid of approximately 8 mm diameter to create an inductance and soldering a trimmer capacitor (Oxley Developments Ltd, UK) across the ends of the exposed coaxial shield to form a high impedance parallel resonant circuit [20], which was then tuned to 200 MHz.

The transmit-only saddle coil is tuned and matched by 5.1 pF fixed non-magnetic ceramic capacitors (American Technical Ceramics, USA) and non-magnetic trimmer capacitors (Oxley Developments Ltd, UK), adjusted from outside the magnet via long fiberglass rods. It is driven by the MRI system's RF power amplifier (M3200, American Microwave Technology, USA) via an active decoupling circuit [21]. Three PIN diodes (5082–3188, Agilent Technologies, USA) are wired in series to form an RF switch, which is connected to the saddle coil through a coaxial line of length λ [21].

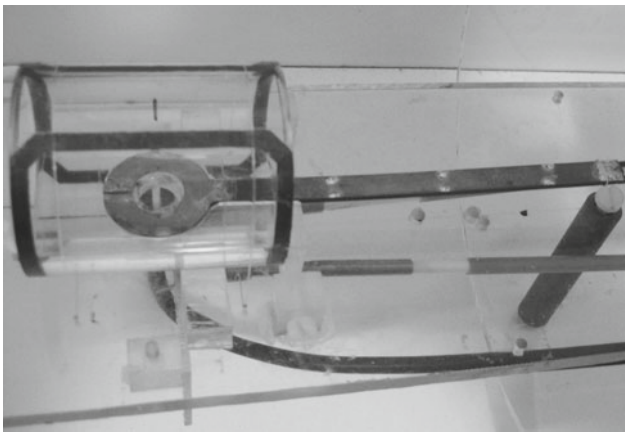

Fig. 4 The 20 mm diameter stripline surface coil positioned inside the 50 mm diameter transmit-only saddle coil

During transmission the PIN diodes conduct and RF pulses are delivered to the transmit coil via the matched line. During reception, the PIN diodes behave like an open circuit so that any unwanted noise from the RF amplifier is blocked and also, because the line becomes unmatched, the transmit coil is detuned [21]. The TTL transmit gate output from the SMIS MRI console is fed through a Schmitt Trigger opto-isolator (H11N3-M, Fairchild Semiconductor, USA) to reduce RF interference and then buffered by hex inverters wired in parallel (74VHC04N, Fairchild Semiconductor, USA) to provide sufficient drive current for the PIN diodes. For imaging experiments, the stripline surface coil was mounted on an acrylic base that fits inside the saddle coil and ensures orthogonality between the transmit and receive fields, helping to minimise magnetic coupling effects. Figure 4 shows the assembled 20 mm diameter stripline surface coil receiver fitted inside the 50 mm diameter saddle coil transmitter.

Actively decoupled copper wire surface coil

The new stripline surface coil was compared with a conventional, actively decoupled wire loop surface coil. This conventional surface coil is manufactured from 2 mm diameter copper wire made into a single-turn 20 mm diameter loop. The coil is tuned by a 5.1 pF, non-magnetic chip capacitor (American Technical Ceramics, USA) located at the loop and a non-magnetic trimmer (Oxley Developments Ltd, UK). It is capacitively matched to 50 Ω using a balanced matching circuit [14] and is connected to the MRI system's 50 Ω preamplifier (AU-1114, MITEQ, USA) via a cable trap similar to the one described before. A PIN diode-based network provides active detuning during excitation pulses [21]. For imaging experiments, the copper-wire surface coil was used with the actively decoupled saddle coil described above.

Results

Unloaded and loaded Q-factors of the actively decoupled copper-wire surface coil ($L = 37$ nH) and the new stripline surface coil ($L = 39$ nH) were measured using a coupling loop connected to the network analyser in reflection mode. Tissue-equivalent loading was provided by a 20 mm diameter tube filled with a solution of $NiSO_4$ (48 mM/l) and NaCl (9 g/l). Detuning from resonant frequency in the presence of the conductive sample was also measured and the results are shown in Table 1. A 0.5 mm-thick PTFE spacer was placed between samples and the copper-wire surface coil for these measurements and subsequent imaging experiments to ensure a similar "lift-off effect" [16] to the stripline coil and therefore aid meaningful comparison between the two coils.

To assess the spatial distribution of the RF fields from the wire and stripline surface coils, B_1 maps were generated using the two coils in transmit/receive mode. For these experiments, the stripline surface coil was matched to a 50 Ω transmit/receive switch via a tuning and matching network [22]. The RF amplifier power was increased by 6 dB (4 times) relative to that required for a perfect 90° flip angle, obtained for a global maximum signal [5], and spin echo images were acquired of a flat, 20 mm rectangular cross-section phantom filled with $NiSO_4$ (48 mM/l) and NaCl (9 g/l) solution.

The regions corresponding to flip angles of $\pi/2 + n\pi$ ($n = 0, 1, 2, 3, \ldots$) will produce maximum signal resulting in bright bands, while the regions corresponding to flip angles of $\pi + n\pi (n = 0, 1, 2, 3\ldots)$ will produce minimum signal, resulting in dark bands. In this way, a contour map of the spatial distribution of the RF field is generated [23].

Because the stripline coil is matched to 50 Ω its Q-factor will be halved, so this experiment will not reflect the true sensitivity of the coil when used as a receive-only coil with the MOSFET preamplifier. However the resulting axial and sagittal B_1 maps, shown in Fig. 5, provide a clear representation of the RF fields from the copper-wire and the stripline surface coils.

Transverse images of the 20 mm diameter $NiSO_4$/saline sample described above were also acquired using a spin echo sequence for the two types of surface coils in receive-only

Table 1 Unloaded Q, loaded Q and frequency shifts under loading for the actively decoupled copper-wire surface coil and stripline surface coil

	Actively decoupled copper-wire surface coil	Duroid 5880 stripline surface coil
Unloaded Q	206	182
Loaded Q	138	132
Frequency shift (MHz)	–0.5	–0.2

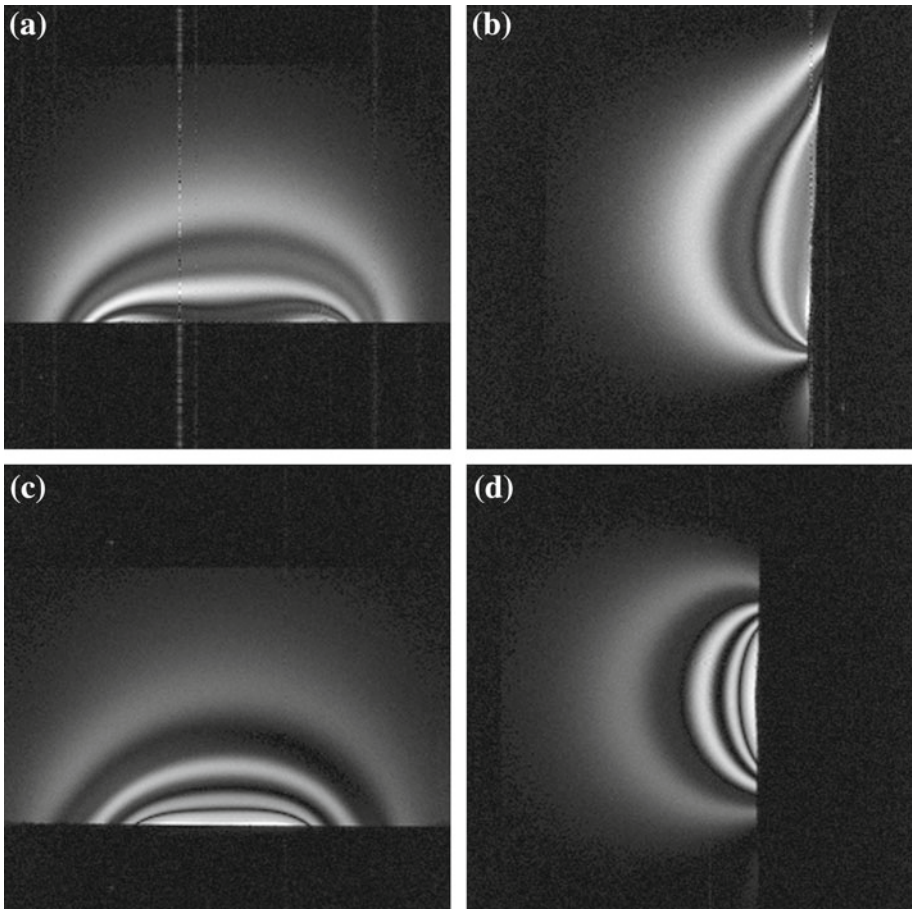

Fig. 5 Axial and sagittal B_1 maps for the actively decoupled copper-wire surface coil (**a, b**) and stripline surface coil (**c, d**). (256 × 256 pixels, receive bandwidth = 20 kHz, $N_A = 2$, field of view = 40 mm, slice thickness = 1 mm, TR=500 ms, TE = 35 ms)

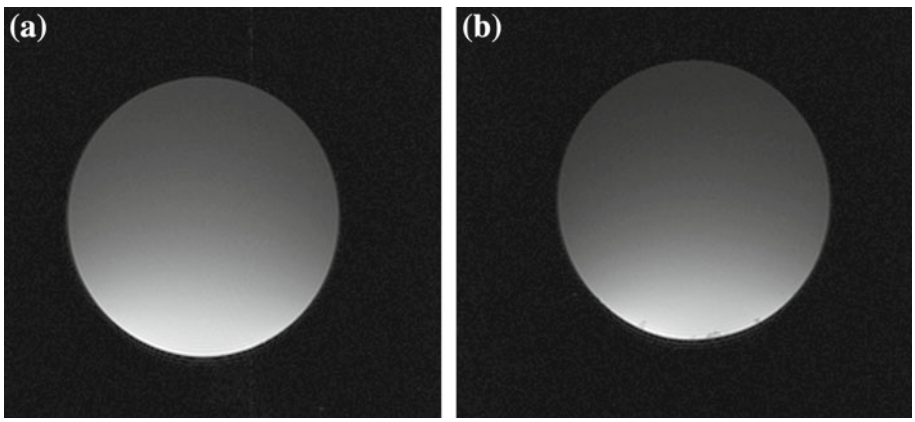

Fig. 6 Transverse slice of the cylindrical phantom acquired with the actively decoupled copper-wire surface coil (**a**) and the stripline surface coil (**b**) (256 × 256 pixels, receive bandwidth = 20 kHz, $N_A = 2$, field of view = 30 mm, slice thickness = 1 mm, TR = 500 ms, TE = 30 ms, 5-lobe sinc pulse of 4000 μs duration)

mode, using the high input impedance MOSFET preamplifier for the stripline surface coil, and are shown in Fig. 6. Before imaging the stripline surface coil was tuned for maximum signal by adjusting C_t while observing the FID from a pulse-and-acquire experiment. This was the only adjustment required to the receiver.

Vertical SNR profiles through these images are plotted in Fig. 7 [24].

Discussion

The stripline surface coil exhibits a similar loaded Q-factor to the actively decoupled copper-wire surface coil (132 rather than 138) while the ratio of unloaded to loaded Q-factor is lower (1.4 rather than 1.5). Coil de-tuning in the presence of the conductive sample, which serves as indication of the amount of dielectric losses [14,25], is reduced in the case of

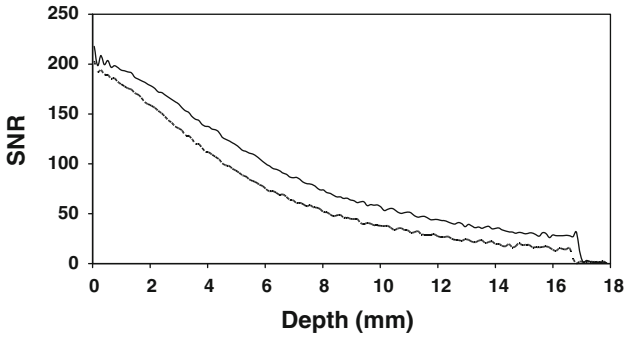

Fig. 7 Vertical SNR profiles for the images shown in Fig. 6a (*solid line*) and 6b (*dashed line*)

the stripline coil (−0.2 rather than −0.5 MHz), verifying that dielectric losses in the presence of the conductive sample are low (Table 1).

The sagittal B_1 map from the copper-wire surface coil is asymmetrical with respect to the coil axis (Fig. 5b); however, by contrast, no such distortion appears in the image from the stripline coil (Fig. 5d). The B_1 distortion is probably associated with the pre-tuning capacitor used in the copper-wire surface coil. The stripline surface coil does not use lumped tuning and matching elements; thus its B_1 profile remains undistorted in these regions.

The copper-wire surface coil (solid line) has marginally better SNR than the new stripline surface coil (dashed line) (Fig. 7). For example, at distance 8 mm from the coil plane, which should cover most of a mouse brain, the SNR of the stripline surface coil is reduced by 30% when compared to that from the wire loop surface coil. Use of a thicker dielectric, however, may improve the depth penetration of the stripline surface coil so that its SNR equals or even exceeds that of the copper-wire one [9]. However, care should be taken because a wider spacing between the two ground planes will result in a decrease of the TEM mode cut-off frequency. The cut-off frequency for the lowest order TEM mode of the stripline configuration described in this work is 238 GHz and a doubling of spacing to 3.2 mm, would only reduce the cut-off frequency to 184 GHz [13], still significantly above the 200 MHz Larmor frequency at 4.7 T.

Conclusion

We have developed a coil system comprising a stripline receive-only surface coil and actively decoupled, transmit-only saddle coil for imaging studies of the mouse brain at 4.7 T. Because the stripline surface coil is fully shielded, it shows very little electrical interaction with conductive samples, thus minimising dielectric losses and requires no further tuning adjustments after initial set up. Also, because the open end of the stripline surface coil presents a high impedance it may be directly connected to the input of a MOSFET preamplifier without using a matching network [1]. The elimination of tuning and matching adjustments makes the coil easy to use and helps to reduce preparation time during scanning. Moreover, because the stripline surface coil is entirely fabricated using PCB techniques, with no external lumped components, the structure is compact and robust, electrically reliable and easy to clean. By comparison, it can be difficult to manufacture TLR surface coils from thick coaxial cables [1] especially at the small diameters required for a mouse brain.

The stripline surface coil described here shows an undistorted B_1 map in sagittal views but has limited axial penetration when compared to a conventional copper-wire surface coil and thus exhibits slightly poorer SNR. We believe, though, that if a thicker substrate material were used [9] then this type of stripline surface coil configuration could match the performance of a conventional actively decoupled, loop surface coil, while maintaining the advantages described above. Further work could also investigate methods of adjusting the optimum source impedance of the MOSFET preamplifier [17,18] to improve matching with the open end of the stripline coil, with the aim of further improving the SNR.

Acknowledgments We thank Dr Sebastian W. Rieger for his initial evaluation of coaxial cable TLR coils and the MOSFET preamplifier. We also thank Mr. Peter W. Frew, Mr. Edward C. Stevenson and Mr Philip G. Mullen of the BioMedical Physics workshop for fabricating RF coil components. This work was supported by a studentship funded by WisTa Laboratories Ltd.

References

1. Zabel HJ, Bader R, Gehrig J, Lorenz WJ (1987) High-quality MR imaging with flexible transmission line resonators. Radiology 165(3):857–859
2. Wu B, Zhang X, Qu P, Shen GX (2007) Capacitively decoupled tunable loop microstrip (TLM) array at 7 T. Magn Reson Imaging 25(3):418–424
3. Lee RF, Hardy CJ, Sodickson DK, Bottomley PA (2004) Lumped-element planar strip array (LPSA) for parallel MRI. Magn Reson Med 51(1):172–183
4. Adriany G, Vande Moortele PF, Wiesinger F, Moeller S, Strupp JP, Andersen P, Snyder C, Zhang X, Chen W, Pruessmann KP, Boesiger P, Vaughan T, Ugurbil K (2005) Transmit and receive transmission line arrays for 7 Tesla parallel imaging. Magn Reson Med 53(2):434–445
5. Burian M, Hájek M (2004) Linear microstrip surface coil for MR imaging of the rat spinal cord at 4.7 T. Magn Reson Mater Phys Biol Med 17(3):359–362
6. Lee RF, Westgate CR, Weiss RG, Newman DC, Bottomley PA (2001) Planar strip array (PSA) for MRI. Magn Reson Med 45(4):673–683
7. Stensgaard A (1997) Planar quadrature coil design using shielded-loop resonators. J Magn Reson 125(1):84–91
8. Wu B, Zhang X, Qu P, Shen GX (2006) Design of an inductively decoupled microstrip array at 9.4 T. J Magn Reson 182(1):126–132

9. Zhang X, Ugurbil K, Chen W (2001) Microstrip RF surface coil design for extremely high-field MRI and spectroscopy. Magn Reson Med 46(3):443–450
10. Zhang X, Zhu X-H, Chen W (2005) Higher-order harmonic transmission-line RF coil design for MR applications. Magn Reson Med 53(5):1234–1239
11. Zhang X, Ugurbil K, Sainati R, Chen W (2005) An inverted-microstrip resonator for human head proton MR imaging at 7 tesla. IEEE Trans Biomed Eng 52(3):495–504
12. Konishi Y (1998) Microwave electronic circuit technology. Marcel Dekker Inc., New York
13. Bahl IJ, Garg R (1978) A designer's guide to stripline circuits. Microwaves: 90–97
14. Mispelter J, Lupu M, Briguet A (2006) NMR Probeheads for biophysical and biomedical experiments. Imperial College Press, London
15. Rogers Corporation (2010) RT/duroid®5870 /5880 High frequency laminates datasheet. http://www.rogerscorp.com/documents/606/acm/RT-duroid-5870-5880-Data-Sheet.aspx. Accessed 20-02-2010
16. Suits BH, Garroway AN, Miller JB (1998) Surface and gradiometer coils near a conducting body: the lift-off effect. J Magn Reson 135(2):373–379
17. Wilson M, Ford SR (eds) (2008) The ARRL handbook for radio communications. ARRL the national association for amateur radio, Newington
18. Philips Semiconductors/NXP Semiconductors (2010) BF981 silicon N-channel dual gate MOS FET datasheet. http://www.datasheetarchive.com/BF981-datasheet.html. Accessed 20-02-2010
19. Alecci M, Jezzard P (2002) Characterization and reduction of gradient-induced eddy currents in the RF shield of a TEM resonator. Magn Reson Med 48(2):404–407
20. Peterson DM, Beck BL, Duensing GR, Fitzsimmons JR (2003) Common mode signal rejection methods for MRI: reduction of cable shield currents for high static magnetic field systems. Concepts Magn Reson Part B: Magn Reson Eng 19B(1):1–8
21. Mellor P, Checkley D (1995) Active coil isolation in NMR imaging and spectroscopy using PIN diodes and tuned transmission line: a practical approach. Magn Reson Mater Phys Biol Med 3(1):35–40
22. Pop-Fanea L, Vallespin SN, Hutchison JMS, Forrester JV, Seton HC, Foster MA, Liversidge J (2005) Evaluation of MRI for in vivo monitoring of retinal damage and detachment in experimental ocular inflammation. Magn Reson Med 53(1):61–68
23. Zelaya FO, Roffmann WU, Crozier S, Teed S, Gross D, Doddrell DM (1997) Direct visualisation of B1 inhomogeneity by flip angle dependency. Magn Reson Imaging 15(4):497–504
24. Henkelman RM (1985) Measurement of signal intensities in the presence of noise in MR images. Med Phys 12(2):232–233
25. Redpath TW, Hutchison JMS (1984) Estimating patient dielectric losses in NMR imagers. Magn Reson Imaging 2(4):295–300